Nuclear Materials and Energy 19 (2019) 59–66

Contents lists available at ScienceDirect

Nuclear Materials and Energy

journal homepage: www.elsevier.com/locate/nme

First mirror test in JET for ITER: Complete overview after three ILW campaigns

Sunwoo Moon[a,*], P. Petersson[a], M. Rubel[a], E. Fortuna-Zalesna[b], A. Widdowson[c], S. Jachmich[d], A. Litnovsky[e], E. Alves[f], JET Contributors[g,1]

[a] Royal Institute of Technology (KTH), SE-10044 Stockholm, Sweden
[b] Warsaw University of Technology, 02-507 Warsaw, Poland
[c] Culham Centre for Fusion Energy, Culham Science Center, Abingdon, OX14 3DB, UK
[d] Laboratory for Plasma Physics, Ecole Royale Militaire-Koninklijke Militaire School, 1000 Brussels, Belgium
[e] Institut for Climate and Energy Research (IEK-4), Forschungszentrum Jülich, 52425 Jülich, Germany
[f] IPFN, Instituto Superior Técnico, Universidade de Lisboa, 1049-001, Lisboa, Portugal
[g] EUROfusion Consortium, JET, Culham Science Centre, OX14 3DB, Abingdon, UK

ARTICLE INFO

Keywords:
JET
First Mirror Test
Diagnostic mirrors
Erosion-deposition
ITER-like Wall

PACS:
52.40 Hf

ABSTRACT

The First Mirror Test for ITER has been carried out in JET with mirrors exposed during: (i) the third ILW campaign (ILW-3, 2015–2016, 23.33 h plasma) and (ii) all three campaigns, i.e. ILW-1 to ILW-3: 2011–2016, 63,52 h in total. All mirrors from main chamber wall show no significant changes of the total reflectivity from the initial value and the diffuse reflectivity does not exceed 3% in the spectral range above 500 nm. The modified layer on surface has very small amount of impurities such as D, Be, C, N, O and Ni. All mirrors from the divertor (inner, outer, base under the bulk W tile) lost reflectivity by 20–80% due to the beryllium-rich deposition also containing D, C, N, O, Ni and W. In the inner divertor N reaches 5×10^{17} cm^{-2}, W is up to 4.3×10^{17} cm^{-2}, while the content of Ni is the greatest in the outer divertor: 3.8×10^{17} cm^{-2}. Oxygen-18 used as the tracer in experiments at the end of ILW-3 has been detected at the level of 1.1×10^{16} cm^{-2}. The thickness of deposited layer is in the range of 90 nm to 900 nm. The layer growth rate in the base (2.7 pm s^{-1}) and inner divertor is proportional to the exposure time when a single campaign and all three are compared. In a few cases, on mirrors located at the cassette mouth, flaking of deposits and erosion occurred.

1. Introduction

Metallic mirrors will be essential components of all optical diagnostics and imaging techniques in next-step fusion devices. Transmission of light signals will rely on mirrors which are the first components of periscope-shaped systems to guide the light in the shielding block. According to the current plan, in the International Thermonuclear Experimental Reactor (ITER) there will be about 80 first mirrors [1]. Therefore, their performance is crucial for reliable plasma diagnosis and safe operation. The main concern is the reflectivity degradation by phenomena arising from plasma-surface interaction (PSI): erosion and deposition. For that reason, a broad research program has been carried out both in tokamaks and in laboratories: exposures of mirrors made of different materials, detailed surface studies, development of cleaning and protection methods [2–6].

First Mirror Test (FMT) at JET for ITER started in 2002 with planning of mirror location and the design of test specimens and mirror carriers (cassettes with channels) [7]. The first exposure took place during the 2005–2007 campaign in the presence of carbon wall, i.e. in JET-C [8]. They were followed by another campaign in that surrounding [9]. All reported results on mirror testing in JET-C have clearly shown complete degradation of optical performance of all specimens from the divertor and also mirrors located in channels of the cassette on the main chamber wall [8, 9]. Two campaigns in JET-C were then followed by three experiments in JET with the ITER-like wall (JET-ILW) [10–12]. During these five campaigns over 100 mirrors were tested.

The aim of this work is to provide an overview of results obtained from the mirrors exposed during: (i) the third ILW campaign (ILW-3, 2015–2016) and (ii) all three campaigns (ILW1-3, 2011–2016). This is

* Corresponding author.
E-mail address: sunwoo@kth.se (S. Moon).
[1] See author list in the paper, X. Litaudon et al., Nucl. Fusion, 57 (2017) 102001.

https://doi.org/10.1016/j.nme.2019.02.009
Received 20 July 2018; Received in revised form 17 January 2019; Accepted 6 February 2019
Available online 15 February 2019

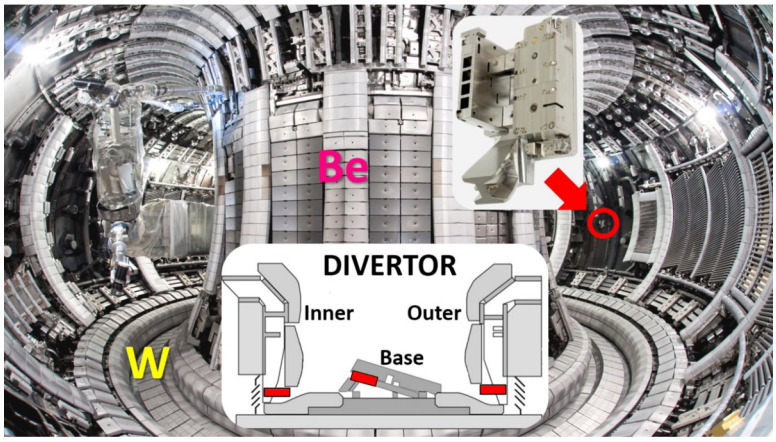

Fig. 1. View inside the JET-ILW vacuum vessel with beryllium limiters and tungsten divertor. The location of cassettes with test mirrors in the divertor is shown schematically: rectangles in the shadowed part of the inner and outer leg and under the load bearing tile in the divertor base. A wall bracket with mirrors in a cassette and the installation place in the main chamber is indicated.

the first report on comparison result of mirrors exposed in a single campaign and the whole operation period under ILW conditions, i.e. tungsten in the divertor and beryllium in the main chamber wall [13, 14].

2. Experimental

The test mirror in JET is a poly-crystalline molybdenum 1 cm^3 cube with a polished surface on one-side. Fifteen mirrors were exposed during ILW-3, while ten others were facing plasma during all three ILW campaigns ILW1-3. Test mirrors were placed in pan-pipe shaped cassettes installed on the main chamber wall (5 pieces for ILW-3) and in the divertor: base under the bulk tungsten tile (4 for ILW-3, 4 for ILW1-3) [10] and in shadowed regions of the inner (3 for ILW-3, 3 for ILW1-3) and outer legs (3 for ILW-3, 3 for ILW1-3) [7], as shown in Fig. 1. The cassettes have several channels (2, 3 or 5) each housing one mirror with a small holder to fix the mirror in the channel. For a given cassette one mirror was placed at the mouth (0.0 cm), while other specimens were sitting deeper, e.g. 1,5, 3.0 cm, from the entrance, thus at the longer distance from plasma. Standard channels have square 1 × 1 cm cross-sections, as shown in [7] and it also can be perceived in Fig. 2: first channel on the left. This has been the feature of all cassettes in the divertor. Only the construction of a five-way cassette installed at main chamber during ILW-3 was designed differently in order to test protection of mirrors against deposition by using baffled structures; a series of hollow (0.57 cm diameter) baffles, as shown in Fig. 2. One mirror placed at the entrance, two mirrors in baffled channels (1.5 and 4.5 cm) and, for comparison, two others were in straight channels of circular cross-section, also 0.57 cm in diameter.

The exposure time of all three ILW campaigns (ILW1-3) was 63.52 h of plasma operations including 19.67 h of limiter discharges and 43.85 h of X-point plasma. For the last single campaign (ILW3), this was 23.33 h, 4.86 h and 18.47 h, respectively. The total energy input was 245 GJ during ILW-3 and 496 GJ in all three campaigns. According to the assessment presented in [15] these huge numbers would correspond around 550 ITER discharges of 400 s duration, but only to around 15 if scaled by energy input or even less than two in terms of the divertor fluence.

Besides the total operation time there are other factors to be taken into account: (i) strike point distribution, especially in ILW-3, which is important for the divertor mirrors; (ii) wall conditioning during campaigns which could influence predominantly mirrors from the main chamber. The strike point in ILW-3 was mainly on Tile 3 (vertical target in the inner divertor) and Tile 6 which is in the base of the outer divertor. Wall conditioning by glow discharge (GD) in deuterium comprised: 564 h, 517 h and 1027 h in consecutive campaigns, ILW-1 to ILW-3, respectively. GD cleaning is mentioned here though earlier results from ILW-1 have not indicated any difference in optical performance of main chamber mirrors exposed in two types of cassettes: one with a magnetic shutter (construction details in [7] and the seconds with channels fully open to plasma at all times [10].

Optical properties of mirrors were examined before and after plasma exposure. Total and diffuse reflectivity measurements in the wavelength range of 400–1600 nm for all ILW-3 and ILW1-3 mirrors were performed in a glove-box complying with safety procedures for material retrieved from JET, i.e. beryllium- and tritium-contaminated

Fig. 2. Five-way cassette from main chamber wall. From the left: mirror at 0.0 cm at the cassette mouth placed in the standard square channel; 1.5 cm deep circular and baffled channels and a similar set with mirrors at the depth of 4.5 cm.

components [7, 16]. Except three mirrors coated by flaking co-deposits, the reflectivity was determined also in the wavelength range 300–2400 nm by dual-beam spectrophotometer, Lambda 950, Perkin Elmer at the Uppsala University. To determine reflectivity the mirrors were masked leaving a 3 × 5 mm elliptical opening to allow measurements in the central part of each specimen.

Surface composition of mirrors was analyzed by means of accelerator-based ion beam techniques at the 5 MeV Tandem Accelerator Laboratory (Uppsala University, Sweden). Concentration of species was measured using time-of-flight heavy ion elastic recoil detection analysis (ToF-HIERDA) with a 36 MeV $^{127}I^{8+}$ beam. This method gives good depth resolution of a few nm by excellent mass separation [17].

Visual inspection of mirrors was followed by observations with optical microscopy (OM). It is possible to take photos of highly reflective mirror surface by shallow focusing range. Surface morphology of mirrors was examined at the Warsaw University of Technology using scanning electron microscopy (SEM, Hitachi SU-8000 FE-SEM). This was combined with energy-dispersive x-ray spectroscopy (EDS, Thermo Scientific Ultra Dry) enabling also beryllium detection. That feature is of great importance in studies of Be dust, splashes and mixed co-deposits. The surface roughness was determined by the atomic force microscopy (AFM), Bruker FastScan scanning probe microscope at the Royal Institute of Technology.

3. Results and discussion

3.1. Mirrors from divertor

3.1.1. Visual inspection

Images in Fig. 3(a)-(d) show the appearance of several mirrors from the divertor. There are three clear cases. On majority of divertor mirrors, like those in Fig. 3(a) and (b), there are colorful patterns indicating inhomogeneous deposition. Only in a few cases, on mirrors located at the cassette mouth, flaking and peeling-off of deposits occurred, like in Fig. 3(c). On the contrary, surface of the mirror at 0.0 cm on outer divertor, Fig. 3(d), was mostly eroded by plasma, while the other mirrors from outer divertor were coated with deposits. It should be stressed that the case of erosion on the divertor mirror has been found for the first time in all tests at JET-C and JET-ILW. The plausible reason for erosion is related to the strike point position on Tile 6 at the end of ILW-3. However, the other outer divertor mirror got a flaking co-deposit.

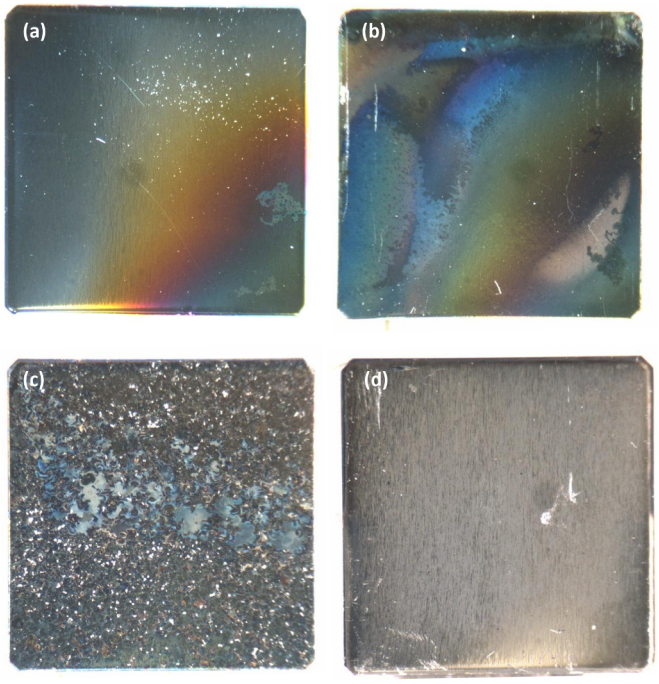

Fig. 3. Optical microscopy photos of mirrors from (a) divertor base at 1.5 cm after ILW-3; (b) divertor base at 1.5 cm after three campaigns (ILW1-3), (c) flaking layer on the inner divertor mirror at 0.0 cm after ILW1-3 and (d) eroded surface of the outer divertor mirror 0.0 cm after IlW-3.

3.1.2. Reflectivity

Graphs in Fig. 4(a)-(f) show total reflectivity of all divertor mirrors exposed during ILW-3 only (Fig. 4a-c) and during all three periods ILW1-3 (Fig. 4d-f). Initial reflectivity of the Mo mirror is plotted on all graphs for comparison to post-exposure values. One may perceive that in three cases (Fig. 4a, d, e) the plots for mirrors at the entrance to respective cassettes are shown only in the spectral range from 400 to 1600 nm. These are surfaces with flaking co-deposited layers. One perceives individual differences between respective mirrors, but there are several general features: (i) distinct loss of reflectivity, 20–80% from the initial value, for all mirrors and (ii) stronger loss of optical performance for mirrors exposed during all three campaigns; (iii) specimens with flaking layers, as expected, have the lowest reflectivity of all measured surfaces. The reflectivity of most mirrors is lower in short wavelength (UV and visible) and gradually increased in near infrared (NIR) range. However, there is no general tendency relating the loss of optical properties dependent on the location (depth) in the channel. In the inner divertor, the reflectivity drop is strongest for the mirrors at the cassette entrance, while in the outer mirrors from nearly all positions (with one exception of the eroded surface shown in Fig. 3d) entirely lost reflectivity. No consistency in property degradation with depth in the channel is observed for the divertor base.

The diffuse reflectivity of most mirrors is less than 3% without strong increase in examination range. In a few cases of flaking layers diffuse reflectivity is up to 8%. The only eroded surface from the outer divertor (ILW-3, 0.0 cm, Fig. 3d) is characterized by a significant level of diffuse reflectivity: up to 11% in the UV range and gradual decrease to around 2% at 2500 nm.

Data presented above regarding reflectivity are fully consistent with all results obtained until now in JET-C and ILW.ILW for the divertor mirrors. There have been some differences between specimens, but the general outcome has always been the same: complete loss of reflectivity because the co-deposition covers the optically active layer of Mo (10–20 nm) [18] and this turns mirror to a deposition monitor.

3.1.3. Surface composition

Co-deposits on the mirror surface contain a mixture of materials deposited during the plasma exposure. In Fig. 5, there are two examples of depth profiling with ToF-HIERDA for mirrors from the divertor base at the same depth of 1.0 cm exposed during a single and three campaigns. The main components of the layers are: beryllium (41–50%) and oxygen (35–42%). This could suggest the presence of a beryllium oxide layer with the admixture of H, D, C, N, steel and Inconel constituents (Ni, Cr, Fe) and tungsten. After the ILW-3 campaign following amounts were determined: 1.9×10^{16}(H), 1.3×10^{17}(D), 2.4×10^{16}(C), 4.1×10^{16}(N), 2.1×10^{16}(Ni) and 1.3×10^{16}(W). The concentrations of respective species after ILW1-3 are about 3 times higher. In Table 1 the concentrations of all elements on divertor mirrors are given. It should be stressed that the carbon content is very low, both the total amount and relative to other species, especially Be.

The broad interface between the deposits and substrate can be associated with the averaging of composition in the ion beam spot in HIERDA (5 mm^2) and material mixing during long-term presence of mirrors at elevated temperature in a reactor [10]. Despite that broad interface, the co-deposit thickness can be estimated by the substrate atomic fraction. The deposition thickness is about 220 nm for the single campaign and 610 nm after three campaigns. It is proportional to the plasma exposure time. The assessed layer growth rate is around 2.7 pm s^{-1}. For other mirrors from the base and the inner divertor there is similar proportionality to the exposure time, as that shown in Fig. 6: co-

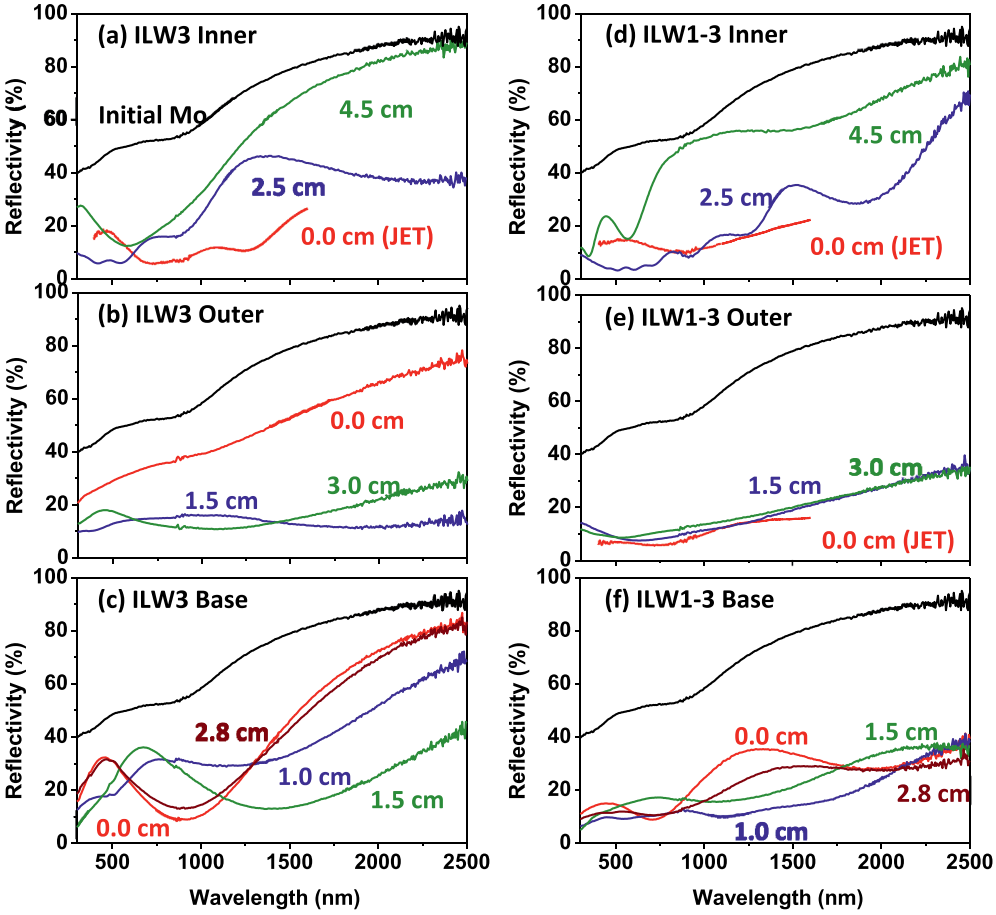

Fig. 4. Total reflectivity of all mirrors from the divertor. Description of positions and respective campaigns is inside the frames. Three mirrors at 0.0 cm with flaking layers are: (a) inner divertor during ILW-3 and (d) ILW1-3; outer divertor after ILW1-3.

deposits thickness is 160–230 nm (ILW-3) and 351–612 nm (ILW1-3) in the base under Tile 5 and in the inner divertor it is 103–323 nm (ILW-3) and 254–680 nm (ILW1-3). However, the layers on the outer divertor mirrors, with the exception of the eroded one, are 2–5 times thicker than those in other locations and, the major contribution comes from the last ILW-3 campaign: 543–681 nm (ILW-3) and 681–818 nm (ILW1-3). The most probable reason is related to the strike point position in ILW-3 on Tile 6 which is near to the outer divertor mirrors. During the ILW-3 the cumulative strike point time on Tile 6 was greater than in ILW-1 and ILW-2. The reflected charge exchange (CX) neutrals on Tile 6 can impact on the mirror surface. In general, the deposition thickness decreases with depth in the cassette channel for the inner and outer divertor, except the eroded surface.

Mirrors belong to a large group of erosion-deposition diagnostic tools (wall probes) in JET [19]. Smooth metal surfaces make them particularly useful in analyses of deposition following tracer experiments performed at the end of ILW-3. Rare isotopes of nitrogen (^{15}N) and oxygen (^{18}O) were injected. This was to assess deposition and retention of nitrogen which is regularly used for plasma edge cooling. In the case of oxygen, the main point was to verify whether the injected tracer would be found only in the outermost region of co-deposits or also in deeper layers. 15,798 mbarl of $^{15}N_2$ (8.5×10^{23} atoms of ^{15}N)

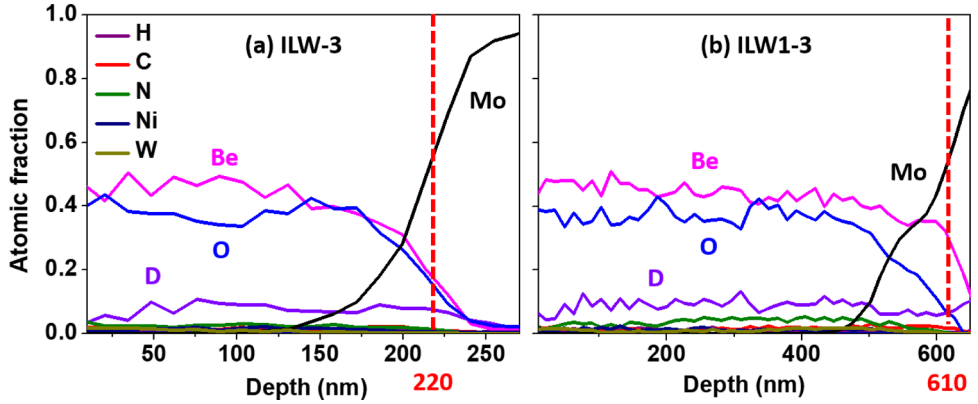

Fig. 5. ToF-HIERDA depth profiling of co-deposits on mirrors from the divertor base at 1.0 cm exposed during (a) ILW-3 and (b) ILW1-3. The vertical dashed lines indicate the thickness of the co-deposits layers.

Table 1
Composition of deposits of divertor mirrors. All numbers are in units of 10^{15} cm^{-2}. Some numbers in bracket were not directly measure in flaking mirrors. They are estimated based on calculation with measured value and same location mirror results.

ILW1-3	Inner	Base	Outer
D	67–1906	161—247	73–1131
Be	854–8625	979–1425	3105–6641
C	60–(159)	50–81	62–(118)
N	214–(555)	72–163	173–(199)
O	481–(1068)	819–1338	960–(1728)
Ni	12–114	28–40	38–379
W	18–425	18–58	8–156
ILW3	**Inner**	**Base**	**Outer**
D	26–738	35–125	4–100
Be	323–2971	495–661	169–2976
C	29–(75)	17–24	46–76
N	61–(248)	32–60	16–139
O	234–(529)	498–574	140–1243
Ni	11–40	15–22	27–281
W	8–147	4–23	7–30

were injected during 35 shots from the gas inlet module (GIM 10) in the outer divertor ring between Tiles 7 and 8, while 524 mbarl of $^{18}O_2$ (0.28×10^{23} atoms of ^{18}O) was puffed from the inlets between Tiles 4 in the inner divertor base (GIM 11). The presence of both tracer gases was detected by ToF-HIERDA on most of the divertor mirrors. The highest contents of oxygen-18 (7.1×10^{15} cm^{-2}) and nitrogen-15 (8.7×10^{15} cm^{-2}) were detected on the top surface of a mirror from the outer divertor, placed at 1.5 cm during ILW-3. A spectrum showing light species including ^{18}O is shown in Fig. 7. The processing of ERDA data is explained in detail in [20]. From the position of the ^{18}O feature (single island) in the spectrum one may infer that the tracer is present only at the very surface of the co-deposit. It means that it took part in the oxidation of species from the outermost layer and did not penetrate to deeper region in the co-deposit.

3.1.4. Dust accumulation on mirror surfaces

In studies of divertor mirrors exposed during ILW-2 a large areal density (300–400 mm^{-2}) of dust particles on surfaces has been found [12]. Micrographs documenting deposits and dust particles obtained in detailed examination of mirrors retrieved after ILW-3 and all three campaigns are shown in Fig. 8(a)–(f). On the stratified deposit shown in Fig. 8(a) one perceives a significant amount of small “dots” which are particles (200 nm–8 μm) representing most categories identified also in earlier regular studies of dust in JET-ILW [12, 21–23]: tungsten ball-like objects with empty interior, droplets of Be, Fe (steel), Ni (Inconel), fragments of Be-rich co-deposits with C, N, O and also small carbon species; the latter are not shown here. A splash of molten tungsten, Fig. 8(e), has been detected for the first time in all ILW dust studies carried until now. The presence of dust is not a feature solely limited to mirrors at the cassette mouth. Particles are detected also on those placed deeper in the channel, though the amount of dust decreases, as expected, with the distance. The presence of dust obviously affects the surface roughness and contributes to the degradation of optical performance degradation.

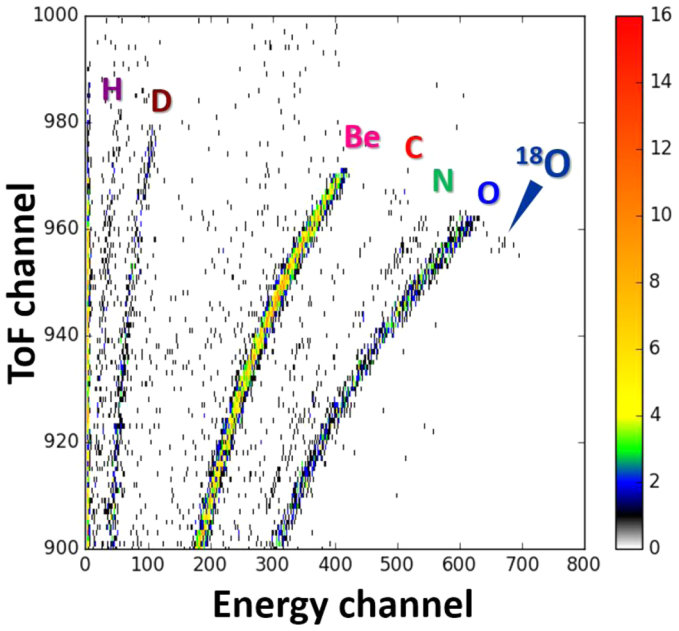

Fig. 7. ToF-HiERDA spectrum for the mirror from the outer divertor at 1.5 cm exposed during ILW3. Oxygen-18 is detected in the outermost layer of the co-deposit.

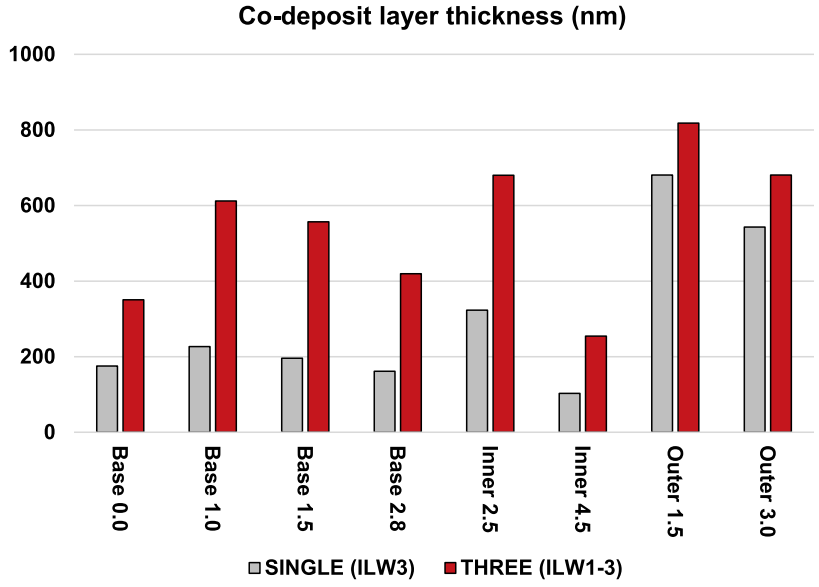

Fig. 6. Thickness of co-deposited layers on divertor mirrors from the single campaign (ILW-3) and three campaigns (ILW1-3).

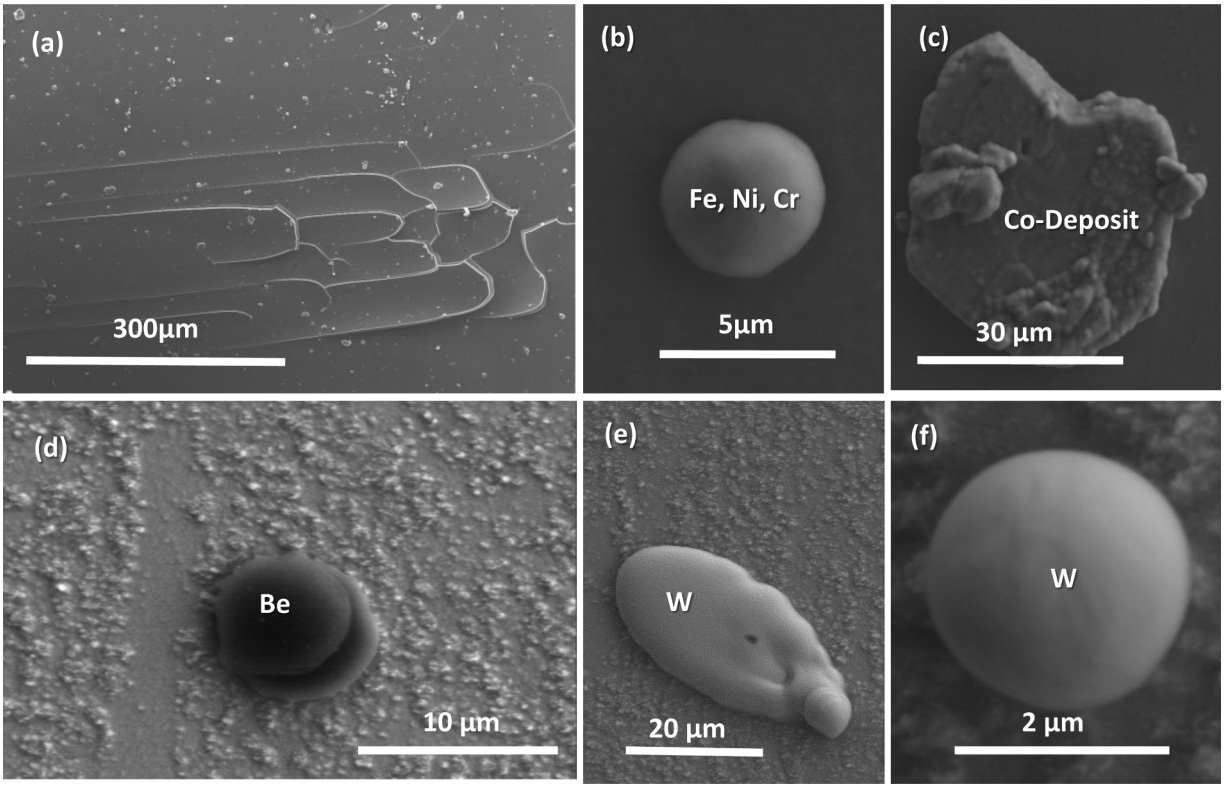

Fig. 8. SEM images of divertor mirror surfaces: (a) general view of the co-deposited layer with a large density of dust particles and (b) steel droplet, outer divertor,1.5 cm, ILW1-3; (c) Be-rich co-deposit with C, N, O outer divertor, 1.5 cm tested during ILW-3; (d) Be droplet on rough co-deposit, (e) tungsten splash and (f) tungsten ball-like structure on the mirror from outer divertor 0.0 cm tested during ILW-3.

3.2. Mirrors from the main chamber

3.2.1. Reflectivity

Graphs in Fig. 9(a) and (b) show respectively the total and diffuse reflectivity of mirrors from the main chamber wall. Initial characteristics are also plotted for comparison. As inferred from Fig. 9(a), the total reflectivity is maintained in the entire examination range. There is a slight relative decrease (2–3%) in near infrared only for the mirror from the cassette entrance (0.0 cm), while there is even relative improvement by 2–10% in the ultra violet and a slight positive trend is in the visible range (< 900 nm) on other mirrors. This improvement is due to the removal of Mo oxide layer which was formed on surfaces before installation of the mirror. This reduction process of the oxide may be associated purely with exposure to hydrogen-rich atmosphere, but it also may indicate erosion by charge exchange neutrals. There is lack of any meaningful difference in reflectivity between mirrors from baffled and circular channels.

As shown in Fig. 9(b) the initial diffuse reflectivity (R_d) was on the level 1.3% in the UV range and 0.7–0.9% in the rest of the spectrum. This component of reflectivity is strongly influenced by the exposure to plasma. R_d values for mirrors located at 1.5 cm and 4.5 cm from the cassette mouth are increased by a factor of up to five in the UV and visible spectrum, while the increase by a factor of two is measured in NIR. No difference can be noticed between mirrors from different types of channels. The strongest change of R_d over the whole spectral range has been determined for the mirrors at 0.0 cm; the reasons are discussed in next paragraphs.

3.2.2. Surface composition

Surface composition of the mirrors is presented in Table 2. The main impurity is carbon at the level of 1–3 × 10^{16} cm^2. These values are similar to those after the ILW-2 campaign [11]. It is immediately stressed that these concentrations are very small (close to the detection limits) corresponding to the layer thickness of 5 nm. The content of other constituents is even smaller. Be, N, O and Ni are on the level of 0.1–2 × 10^{16} cm^{-2}, while deuterium and tungsten are below the

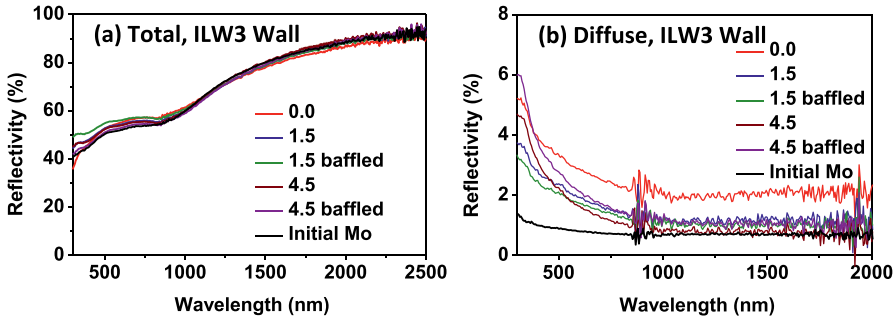

Fig. 9. (a) Total and (b) diffuse reflectivity of mirrors from main chamber wall. The numbers in legend are distance (cm) of mirrors from the cassette entrance. Plots of initial total and diffuse reflectivity are included.

Table 2
Composition of modified layer on wall mirrors. All numbers are in units of 10^{15} cm^{-2}.

ILW3	0.0 cm	1.5 cm	1.5 cm baffled	4.5 cm	4.5 cm baffled
Be	8	2	0	0	2
C	32	12	11	20	10
N	0	4	7	3	2
O	17	5	18	19	10
Ni	0	2	1	0	0

detection limit of 5×10^{13} cm^{-2}. This suggests that the carbon presence may be related not only to tiny amount of deposition from the plasma, but also to other sources including contact with ambient atmosphere during mirror installation, pump-down phase and retrieval procedure.

On the mirror located at the cassette mouth one finds beryllium splashes and small island indicating local oxidation, as shown in images in Fig. 10(a) and (b). There is also tungsten in the form of ball-like structures. The presence of Be splashes is easily explained and attributed to droplets from molten limiters: upper dump plates and outer poloidal. However, deposition of empty tungsten spheres formed most probably by the coagulation of flakes from W coatings on carbon fibre tiles is more difficult to explain. Most such W-coated tiles are in the divertor region, but there is also a belt at the top of the inner wall cladding. One may assume that this is a potential source of tungsten on the main chamber mirrors.

3.2.3. Surface roughness and specific surface features

As written in experimental, the opening in circular and baffled channels was 0.57 cm. Therefore, the surface area exposed to plasma in the case of mirrors located at the depth of 1.5 cm and 4.5 cm was only 25.5 mm^2 (four times less than for other tested mirrors). The optical and surface analyses were carried out in that central part of specimens. The average roughness (R_a) measured with AFM was in the range from 4.70 to 6.20 nm, while for the mirror from the cassette entrance R_a = 8.48 nm. This explains the increased value of diffuse reflectivity of that mirror.

Careful inspection of mirrors from special channels (baffled and circular) revealed one more feature shown in Fig. 11(a) and (b). In the border between the aforementioned central part and the area shadowed by the tube or baffles there are randomly oriented needle-shape structures 30–40 nm in height and about 1–2 μm long. This area has higher roughness (R_a = 8.93 nm) than that measured in the central part, R_a = 4.70 nm, where only some polishing lines are visible. As determined with EDS, “needles” contain mainly Mo. Its signal is accompanied by oxygen, while carbon is the minority species. The origin, formation mechanism and exact composition of the structures are unknown. Truly speaking it is even difficult to find a proper set of techniques to determine conclusively morphology of this very small

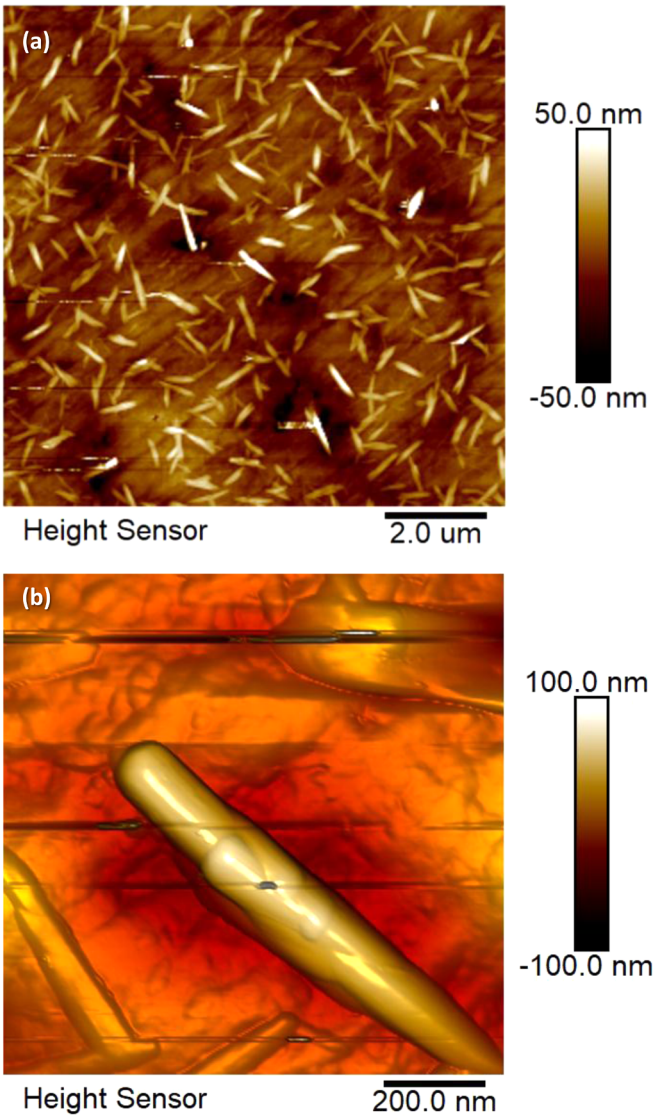

Fig. 11. AFM images of surface: (a) edge of circle area scanned 10 × 10 μm and (b) 1 × 1 μm of wall mirror 4.5 cm baffled.

“needles”. One may very tentatively suggest that they were formed as result of arcing (parasitic discharge) between the mirror and the protecting structure (tube or baffle), but there is no chance to prove it. However, the impact of such structures on the surface roughness leaves no doubts. There is only one, quite obvious, conclusion that the shape and surface finish of diagnostic channels must be carefully tested. This

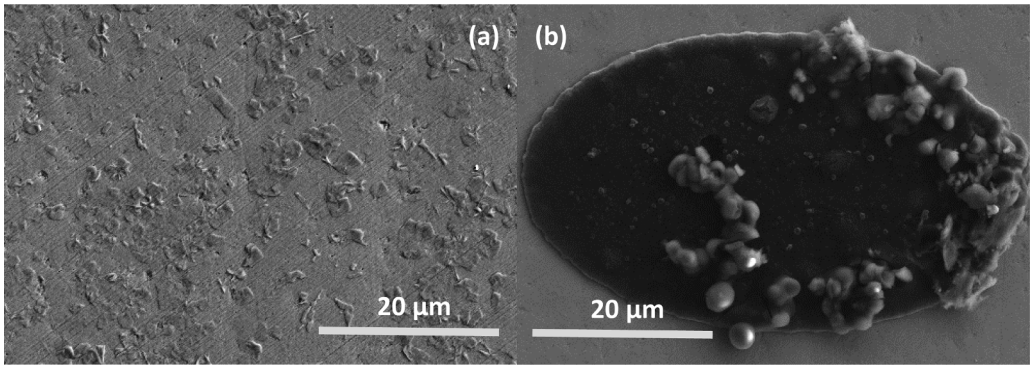

Fig. 10. SEM images of surface: (a) island structures and (b) Be splash on wall mirror from cassettes entrance.

would help elimination of possible negative factors which may influence the surface state of mirrors.

4. Concluding remarks

Results obtained for 15 test mirrors (main wall and divertor) after ILW-3 and 10 divertor mirrors exposed during ILW1-3 provide two sets of messages for diagnostic components in next-step devices. The pessimistic side is such that all tests in the divertor (JET-C and JET-ILW) consistently show that all mirrors, independently on the location completely lose reflectivity because of co-deposition. The growth rate of such layers in JET-ILW with Be as the main component in co-deposits is about 20 times smaller than with carbon PFC, but the final result is equally devastating. If such effects would occur in a reactor with similar intensity and would cause gradual reflectivity degradation during very few discharges, then neither periodic cleaning nor replacement of mirrors would be considered as an effective solution. On the optimistic side one finds main chamber mirrors with a very small change of the total and diffuse reflectivity for mirrors placed deep in the channels. There are still many outstanding points in mirror studies. The list is long, but just to mention a few: tests at other locations, test of various types of channel shape and mirror protection methods, experiments with repetitive exposure/cleaning cycles, demonstration of in-situ cleaning. In parallel, efforts should also be dedicated to the design/development of mirror replacement method.

Acknowledgements

This work has been carried out within the framework of the EUROfusion Consortium and has received funding from the Euratom research and training programme 2014–2018 under grant agreement number 633053. The views and opinions expressed herein do not necessarily reflect those of the European Commission. Work was performed under work package plasma facing components (WPJET2). The support from the Swedish Research Council (VR) under contracts 2017-00643 and 2015-04884 is highly acknowledged.

References

[1] A. Costley, et al., Fusion Eng. Des. 74 (2005) 109.
[2] P. Wienhold, et al., J. Nucl. Mater. 335-339 (2005) 1116.
[3] M. Lipa, et al., Fusion Eng. Des. 81 (2006) 221.
[4] A. Litnovsky, et al., J. Nucl. Mater. 363-365 (2007) 1395.
[5] A. Leontyev, et al., Fusion Eng. Des 86 (2011) 1728.
[6] L. Moser, et al., Phys. Scr. T. 167 (2016) 014069.
[7] M. Rubel, et al., Rev. Sci. Instrum. 77 (2006) 063501.
[8] M. Rubel, et al., J. Nucl. Mater 390-391 (2009) 1066.
[9] M. Rubel, et al., Phys. Scr. T 145 (2011) 014070.
[10] D. Ivanova, et al., Phys. Scr. T. 159 (2014) 014011.
[11] A. Garcia-Carrasco, et al., Nucl. Mater. Energy 12 (2017) 506.
[12] M. Rubel, et al., Phys. Scr. T. 170 (2017) 014061.
[13] G.F. Matthews, et al., Phys. Scr. T. 138 (2009) 014030.
[14] G.F. Matthews, et al., Phys. Scr. T. 145 (2011) 014001.
[15] R.A. Pitts, et al., Plasma Phys. Control. Fusion 47 (2005) B300.
[16] A. Widdowson, et al., Phys. Scr. T. 167 (2016) 014057.
[17] P. Ström, et al., Rev. Sci. Instr. 87 (2016) 103303.
[18] A. Garcia-Carrasco, et al., Nucl. Instr. Meth. B. 382 (2016) 91.
[19] M. Rubel, et al., J. Nucl. Mater 438 (2013) S1204.
[20] H.J. Whitlow, G. Possnert, C.S. Petersson, Nucl. Instr. Meth. B. 27 (1987) 448.
[21] E. Fortuna-Zalesna, et al., Nucl. Mater. Energy 12 (2017) 582.
[22] E. Fortuna-Zalesna, et al., Phys. Scr. T 170 (2007) 014038.
[23] M. Rubel, et al., Fusion Eng. Des. 136 (2018) 579.